Fast-Response Aerodynamic Probes
Paper 11

FAST-RESPONSE TOTAL TEMPERATURE PROBE EXPERIMENTS IN A TURBINE FACILITY

D.R. Buttsworth, T.V. Jones
K.S. Chana

Department of Engineering Science
University of Oxford
Oxford OX1 3PJ

DRA Pyestock
Farnborough, UK

FAST-RESPONSE TOTAL TEMPERATURE PROBE EXPERIMENTS IN A TURBINE FACILITY

D. R. Buttsworth and T. V. Jones
Department of Engineering Science, University of Oxford
Parks Road, Oxford, United Kingdom

K. S. Chana
DRA Pyestock
Farnborough, United Kingdom

ABSTRACT

Experiments using a fast-response flow total temperature measurement technique in a turbine facility are described. Two thin film heat transfer gauges located at the stagnation point of fused quartz substrates are operated at different temperatures in order to determine the flow total temperature. With this technique, no assumptions regarding the magnitude of the convective heat transfer coefficient are made. Thus, the probe can operate successfully in unsteady compressible flows of arbitrary composition and high free-stream turbulence levels without calibrating the probe to determine its heat transfer law. The probe is shown to measure a time-averaged flow total temperature that is in good agreement with thermocouple measurements made downstream of the rotor. Unsteady total temperature measurements are discussed with reference to fast-response aerodynamic probe measurements obtained at the same location downstream of the rotor. It is shown that the overall magnitude of the total temperature and total pressure fluctuations arises mainly due to isentropic effects associated with the extraction of work by the turbine. The present total temperature probe is demonstrated to be an accurate, robust, fast-response device that is suitable for operation in a turbomachinery environment.

NOMENCLATURE

c	specific heat of the substrate (J.kg^{-1}.K^{-1})
h	convective heat transfer coefficient (W.m^{-2}.K^{-1})
k	conductivity of the substrate (W.m^{-1}.K^{-1})
N	rotational speed (rpm)
p	pressure (Pa, bar)
q	surface heat transfer rate (W.m^{-2})
R	radius of the probe, radius of curvature
R	specific gas constant (J.kg^{-1}.K^{-1})
s	entropy (J.kg^{-1}.K^{-1})
t	time
T	temperature of the flow or substrate surface (K)
γ	ratio of specific heats
ρ	density of the flow or substrate material

subscripts

mean	value averaged over the steady flow run time
t	total or stagnation condition
w	value at probe surface (stagnation point)
1	NGV inlet; first probe
2	NGV exit, turbine inlet; second probe
3	turbine exit

superscript

$'$	fluctuating quantitiy

INTRODUCTION

Fast-response total temperature measurements can be made using the aspirating probe first developed by Ng and Epstein (1983) (e.g., Alday et. al, 1993; Van Zante et al., 1994; Suryavamshi et al., 1996). However, the aspirating probe has a number of limitations (e.g., Van Zante et al.) including a restricted frequency response (the claimed bandwidths are generally lower than 40 kHz, Suryavamshi et al., 1996) which may not be sufficient in many applications.

The new fast-response total temperature probe that is discussed in the current paper, has a bandwidth significanly higher than that of the aspirating probe. Furthermore, it offers a number of other advantages including ease of operation and robustness. It is not necessary to calibrate the current probe to determine its heat transfer law (in contrast to hot wire devices). Thus, the new probe is a versatile device that offers a measurement of the total temperature that is independent of the gas composition and other flow parameters. An earlier version of the probe has already been successfully operated in a number of high speed flow situations (Buttsworth and Jones, 1996). The present work represents the first application of the new fast-response total temperature probe in a turbomachinery environment.

PROBE OPERATION

Theoretical Background

The operating principles of this probe have been discussed previously (Buttsworth and Jones, 1996) so only a brief description will presently be given. Fast-response total temperature measurements are obtained by operating two thin film transient heat transfer gauges at two different temperatures. In the present investigation, platinum thin films were painted onto fused quartz substrates as shown in Fig. 1. The thin films are located close to the stagnation point of nominally identical hemispherical probes. Therefore, the convective heat transfer between the flow and the probes is proportional to the temperature difference between the flow *total temperature* and the probe surface temperature. That is,

$$q = h\,(T_t - T_w) \tag{1}$$

The surface temperatures are measured by monitoring the voltage across each of the thin films, and the surface heat fluxes are obtained from either electrical analogues of the heat diffusion process (Oldfield et al., 1982), or numerical methods (Buttsworth, 1996). Since two nominally identical probes are operated in the same flow, the values of h for each probe will be virtually the same. Thus, it is possible to write two equations in two unknowns,

$$q_1 = h\,(T_t - T_{w1}) \tag{2}$$

$$q_2 = h\,(T_t - T_{w2}) \tag{3}$$

which can be solved to obtain the flow total temperature,

$$T_t = T_{w1} + q_1\,(T_{w2} - T_{w1})/(q_1 - q_2) \tag{4}$$

and the convective heat transfer coefficient,

$$h = (q_1 - q_2)/(T_{w2} - T_{w1}) \tag{5}$$

For moderate flow total temperatures, the probe will measure the total temperature because the stagnation enthalpy is conserved as the flow decelerates to the stagnation point and there is virtually no viscous dissipation in the stagnation point boundary layer. At higher flow total temperatures, where gas radiation and dissociation may be significant, the measurement of flow total temperature becomes more involved than is suggested by the above expressions. Total temperature measurements are made without reference to other flow parameters such as the Mach number, pitot pressure, and the flow composition. Thus, the probe offers a measurement of total temperature without needing to know the probe heat transfer law, and therefore many of the calibration issues associated with hot-wire devices are avoided.

a) overview of the probe

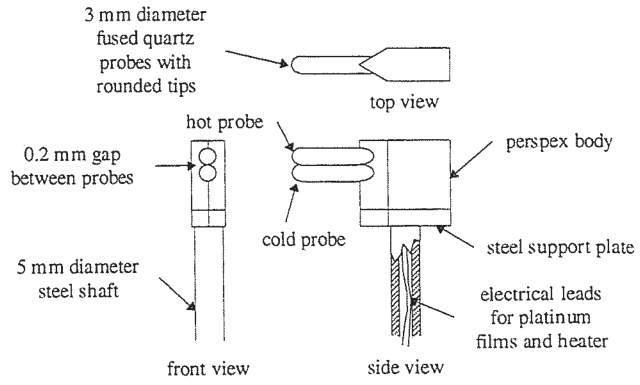

b) details of construction

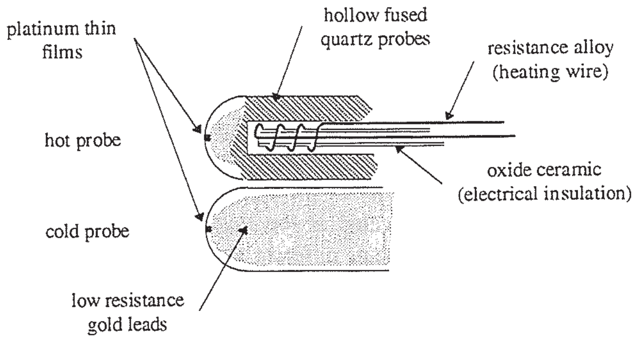

Figure 1. The total temperature probe. a) Overview of the probe configuration; b) details of construction.

Design and Practical Operation

Details of the current implementation of the total temperature probe concept are given in Fig. 1. Both fused quartz probes were hollow, and a small heating element was inserted into the hot probe. The heating element had a resistance of approximately 12 Ω, and, during the turbine experiments, the heater was driven with around 4.6 V (from a battery supply). A temperature increase was experienced at the cold probe due to the heating of the hot probe. To maximize the temperature difference between the hot and cold probes, the heater power supply was only switched on approximately 10 seconds before the run was due to commence. This gave an initial temperature difference between the two films of approximately 50 °C at the start of the flow. Immediately prior to the start of the flow, the temperature of the hot and cold probes was still increasing slightly (however, the rate of change was very small relative to the temperature changes experienced during a run). Such pre-run variations can easily be accounted for when determing the convective heat flux during the run (Buttsworth and Jones, 1996). The heater remained on during the run so that additional transient temperature changes (that would accompany switching the heating power off) did not complicate the interpretation of the temperature changes associated with the convective heating.

a) plan view (at mid-height)

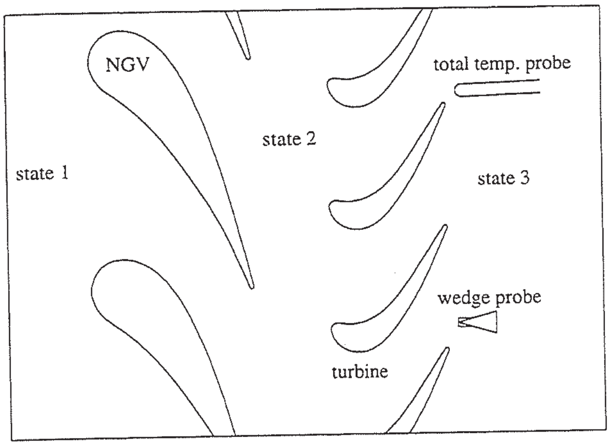

b) side view

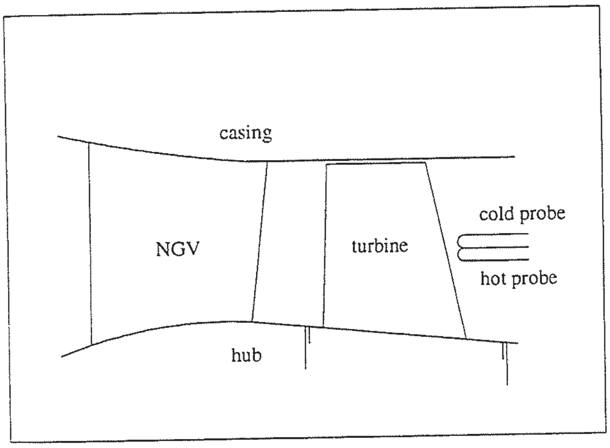

Figure 2. Illustration detailing the instrumentation and its relative location in the turbine experiments (not to scale).

TURBINE EXPERIMENTS

Facility and Instrumentation

Total temperature measurements were made in the Isentropic Light Piston Facility (ILPF) at DRA Pyestock (Hilditch et al., 1994). For the present work, the total temperature probe (Fig. 1) was located approximately 2.5 mm behind the rotor at mid-height as shown in Fig. 2. A photograph of the probe located behind the turbine blades is given in Fig. 3. A fast-response wedge probe was also located at mid-height and at the same distance downstream of the rotor, but at a circumferencial location (relative to the total temperature probe) corresponding to one NGV pitch in the direction of rotation (Figs. 2 and 3). Thus, both the total temperature and the wedge probes should experience a similar flow. Relevant flow parameters given in Table 1 are based on the average conditions measured during the period shown in Fig. 4. The variations given in Table 1 correspond to the maximum and minimum values measured during the current series of experiments.

Table 1. ILPF operating conditions

p_{t1} (Bar)	4.60 (± 1 %)
T_{t1} (K)	445 (± 1 %)
N (rpm)	9564 (± 0.08 %)

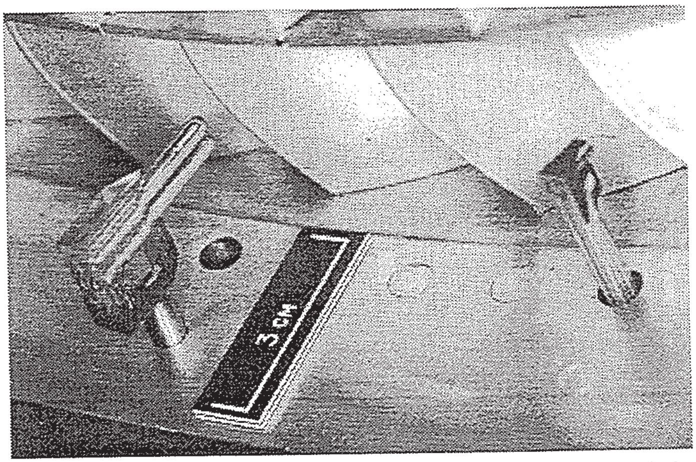

Figure 3. Photograph of the total temperature probe (left) and the wedge probe (right) downstream of the turbine blades.

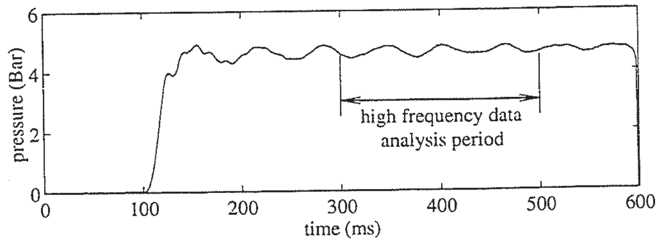

Figure 4. Example of NGV inlet total presssure measurement.

Data Analysis

For each run, the film temperatures were amplified and low-pass filtered (−3dB point around 200 Hz) and then recorded at 500 Hz (referred to as the low sample rate). Heat transfer data from the analogues was low-pass filtered (−3dB point around 200 kHz) and recorded at 1 MHz (referred to as the high sample rate). Using the low sample rate temperature history (Fig. 5a), the time-averaged heat flux level was determined from the finite difference routine (which modelled the spherical probe geometry and variable thermal property effects) and a lateral conduction correction technique which is described elsewhere (Buttsworth, 1996). Time-averaged heat fluxes corresponding to the temperatures in Fig. 5a are shown in Fig. 5b. Time-averaged total temperature results (as given in Fig. 6) were then obtained using the time-averaged film temperature and heat flux results (Fig. 5a and 5b) using Eq. (4).

The analogue heat transfer signals (recorded at 1 MHz) were later conditioned using a high-pass filter (having a −3 dB point at 1 kHz and virtually no attenuation at 10 kHz) and a variable sensitivity that was dependent on the thermal product ($\sqrt{\rho c k}$) at the surface of the substrate (which was a function of the measured surface temperature). An example of the high frequency component of the heat flux processed in this manner is given in Fig. 7. (Spherical and lateral conduction effects do not have a significant influence on the heat transfer fluctuations at such frequencies.) The total heat flux levels were determined from the sum of the heat fluxes obtained using the low and high sample rate data (as illustrated in Fig. 5c). Total temperature fluctuations (as given in Fig. 8) were then determined from the time-averaged film temperature (Fig. 5a) and total heat flux (Fig. 5c) using Eq. (4).

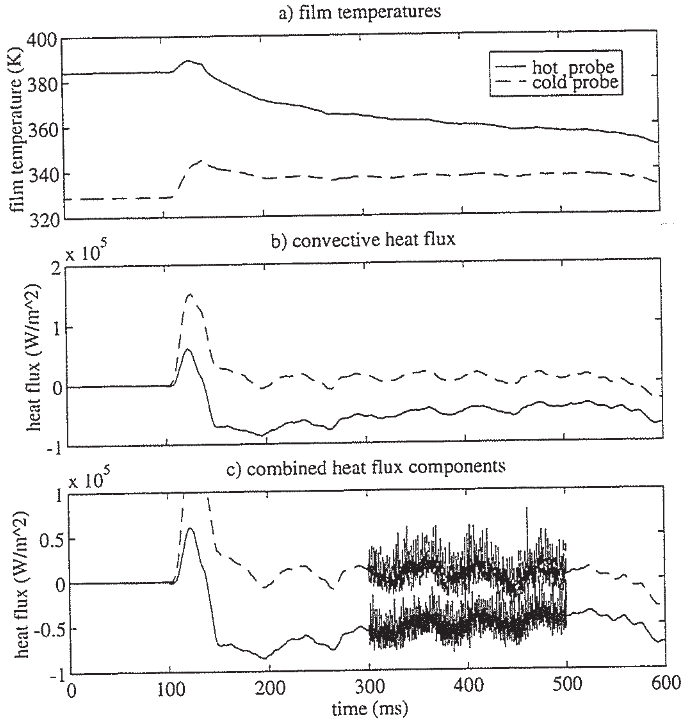

Figure 5. Example of the total temperature probe measurements. a) Thin film temperature histories (low sample rate data); b) Heat flux results obtained from temperature histories (in part a); c) Heat flux data including high and low frequency heat flux components.

Results and Discussion

Time-averaged temperature results from the fast-response total temperature probe are given in Fig. 6 where a comparison is made with thermocouple mesurements obtained using a vented 0.0005" K-type thermocouple probe downstream of the rotor. There is good agreement between the overall level of the fast-response total temperature probe and the thermocouple probe measurements. That is, both measurement techniques indicate a time-averaged flow total temperature during the facility run time of around 340 K. However, it may be noted (see Fig. 6) that the poor frequency response of the thermocouple probe has a significant influence on the temperature measurements even at the relatively low piston oscillation frequency (which is around 15 Hz).

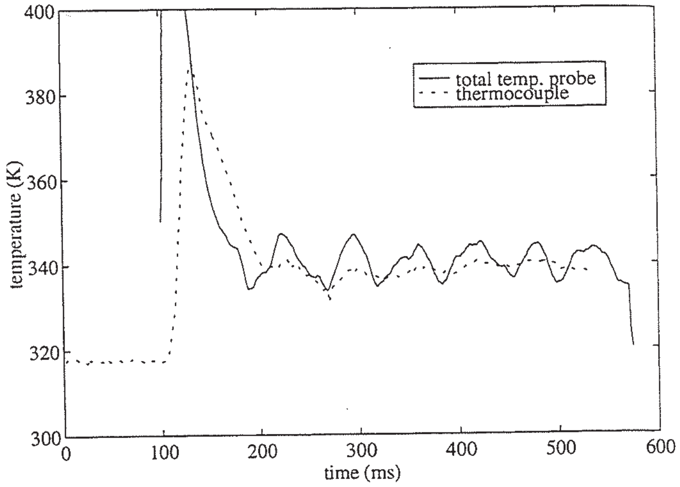

Figure 6. Comparison of fast-response total temperature probe and thermocouple probe results over the facility operation time.

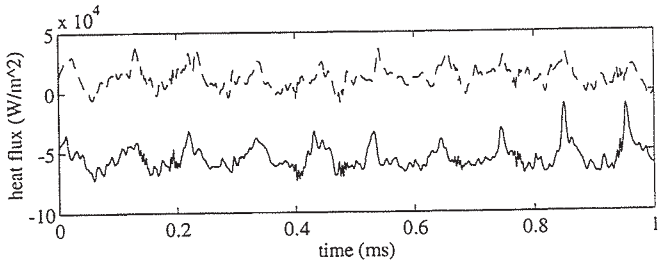

Figure 7. Example of the high frequency heat flux data. (Solid line: hot probe; broken line: cold probe; the dc offsets correspond with the mean heat flux at this point in time.)

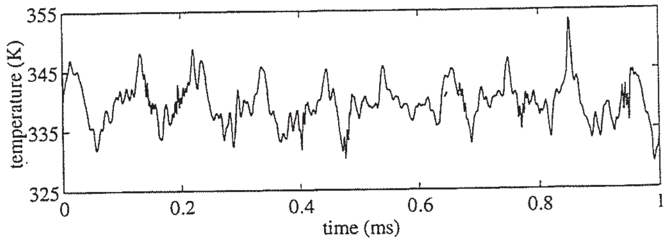

Figure 8. Example of the raw (unaveraged) fast-response total temperature measurements.

By averaging the raw total temperature measurements (e.g., Fig. 8) over 30 rotor revolutions, rotor-averaged total temperature results were obtained for each rotor blade passing event, eight of which are shown in Fig. 9. The corresponding ensemble-averaged total pressure measurements from the wedge probe are given in Fig. 10. The location of the instrumentation relative to the rotor blades at the point given by a "rotor blade index" of 0 (in Figs. 9 to 12) is shown in Fig. 2a.

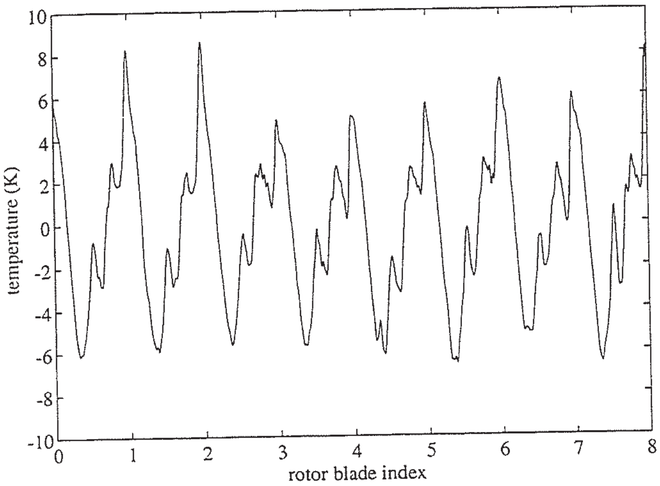

Figure 9. High frequency (rotor-averaged) total temperature results showing 8 blade passing events.

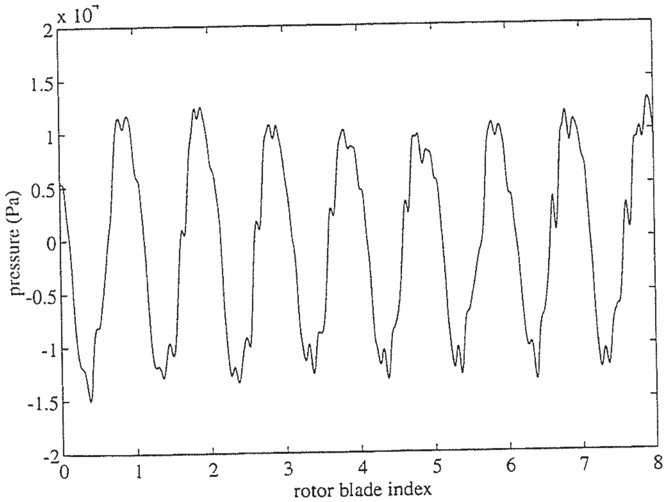

Figure 10. High frequency (rotor-averaged) total pressure results (from the wedge probe) showing 8 blade passing events.

The rotor-averaged temperature and pressure results (e.g., Figs. 9 and 10) were averaged over the total number of blade passing events to yield the pitch-average results as shown in Fig. 11. In this figure, the total temperature and total pressure fluctuations have been normalized using the time-averaged values duing the run, and, in the case of the temperature results, the scaling factor $\gamma/(\gamma-1)$ has also been employed. This scaling factor arises in the context of the 2nd Law of Thermodynamics which gives the expression,

$$s'/R \approx \gamma/(\gamma-1)\; T'/T_{mean} - p'/p_{mean} \qquad (6)$$

where R is the specific gas constant. Three blade passing events are shown in Fig. 11 to provide a clear picture of the periodic nature of the flow, even though the second and third events are identical to the first (since results from all of the rotor blade passing events have been used in the averaging process). The total temperature and wedge probes were located 1 NGV pitch apart (Fig. 2a). As this distance does not correspond exactly with a whole number of rotor pitches, it was necessary to adjust the rotor blade index of pressure measurements relative to the temperature results so that both the temperature and pressure measurements given in Fig. 11 are in phase.

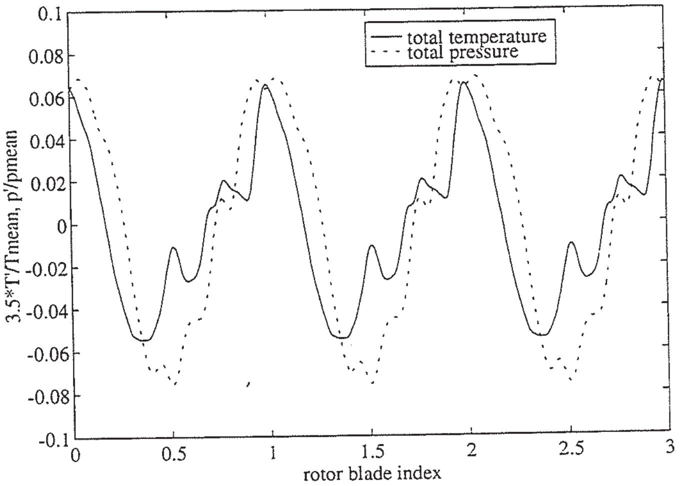

Figure 11. Scaled temperature and pressure fluctuations (pitch-averaged).

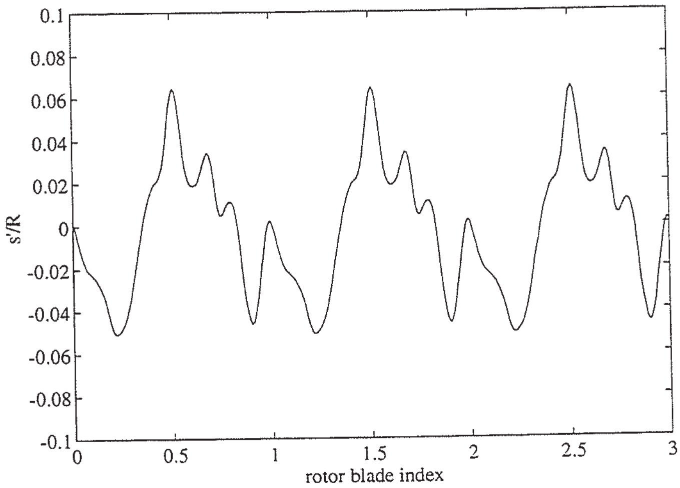

Figure 12. Normalized entropy fluctuatuon from the total temperature probe and total pressure probe measurements.

There exists good agreement between the scaled temperature and pressure results in Fig. 11 in terms of the magnitude and phase of the *large scale* fluctuations. Such agreement suggests that the fluctuations occuring at this location downstream of the rotor arise mainly because of isentropic processes associated with the work extracted by the rotor. It appears that neither the total temperature nor the total pressure measurements alone can be used to identify rotor and NGV wake flow regions. However, it may be possibile to make a positive identification of such regions when the entropy fluctuation is calculated using both the temperature and pressure measurements (Eq. 6). The difference between the scaled temperature and pressure results in Fig. 11 is approximately the normalized entropy fluctuation (Eq. 6) which is shown in Fig. 12. By considering the location of the instrumentation relative to the trailing edge of the rotor (Fig. 2), and the flow transit time from the rotor trailing edge to the instrumentation, the first dip in the entropy fluctuation is tentitively identified as the rotor wake. (A drop in the entropy would be expected within the rotor wake because of the heat lost to the rotor blade.)

CONCLUSIONS

In excess of 15 runs were performed using the total temperature probe in the present turbine facility without any noticible change in the ambient resistance of the films, or degradation of the frequency response. It is concluded that the present total temperature probe is a robust device that is well suited to operation in the turbine facility. Total temperature measurements are obtained without reference to other flow parameters such as the Reynolds number, the Mach number or the flow composition, and thus it offers ease-of-use without compromising its considerable versatility.

ACKNOWLEDGMENTS

The authors wish to thank Mr. T. Godfrey for building the total temperature probe, and Mr. S. J. Anderson for his assistance during the experiments.

REFERENCES

Alday, J., Osborne, D. J., Morris, M. B., Ng, W., and Gertz, J., 1993, "Flow Randomness and Tip Losses in Transonic Rotors," ASME Paper 93-GT-189.

Buttsworth, D. R., 1996, "A Finite Difference Routine for the Solution of Transient One Dimensional Heat Conduction Problems with Varying Thermal Property and Curvature Effects," Department of Engineering Science, University of Oxford, Report.

Buttsworth, D. R., and Jones, T. V., 1996, "A Fast-Response Total Temperature Probe for Unsteady Compressible Flows," ASME Paper 96-GT-350.

Hilditch, M. A., Fowler, A., Jones, T. V., Chana, K. S., Oldfield, M. L. G., Ainsworth, R. W., Hogg, S. I., Anderson, S. J., and Smith, G. C., 1994, "Installation of a Turbine Stage in the Pyestock Isentropic Light Piston Facility," ASME Paper 94-GT-277.

Ng, W. F., and Epstein, A. H., 1983, "High-Frequency Temperature and Pressure Probe for Unsteady Compressible Flows," *Rev. Sci. Instrum.*, Vol. 54, No. 12, 1678-1683.

Oldfield, M. L. G., Burd, H. J., and Doe, N. G., 1982, "Design of Wide-Bandwidth Analogue Circuits for Heat Transfer Instrumentation in Transient Wind Tunnels," 16th Symp. of International Centre for Heat and Mass Transfer, Hemisphere Publishing, pp. 233-257.

Suryavamshi, N., Lakshminarayana, B., and Prato, J., 1996, "Aspirating Probe Measurements of the Unsteady Total Temperature Field Downstream of an Embedded Stator in a Multistage Axial Flow Compressor," ASME Paper 96-GT-543.

Van Zante, D. E., Suder, K. L., Strazisar, A. J., and Okiishi, T. H., 1994, "An Improved Aspirating Probe for Total-Temperature and Total-Pressure Measurements in Compressor Flows," ASME Paper 94-GT-222.